Hindawi
Mathematical Problems in Engineering
Volume 2019, Article ID 8193134, 11 pages
https://doi.org/10.1155/2019/8193134

Research Article

Design and Analysis of Output Feedback Constraint Control for Antilock Braking System with Time-Varying Slip Ratio

Youguo He,[1,2] **Chuandao Lu**,[1] **Jie Shen**,[2] **and Chaochun Yuan**[1]

[1] *Automotive Engineering Research Institute, Jiangsu University, Zhenjiang 212013, China*
[2] *Department of Computer and Information Science, University of Michigan-Dearborn, MI 48128, USA*

Correspondence should be addressed to Youguo He; hyg197715@163.com

Received 15 September 2018; Revised 16 December 2018; Accepted 18 December 2018; Published 3 January 2019

Academic Editor: Tarek Ahmed-Ali

Copyright © 2019 Youguo He et al. This is an open access article distributed under the Creative Commons Attribution License, which permits unrestricted use, distribution, and reproduction in any medium, provided the original work is properly cited.

This paper is concerned with the problem of constraint control for an Antilock Braking System (ABS) with time-varying asymmetric slip ratio constraints. A quarter vehicle braking model with system uncertainties and a Burckhardt's tire model are considered. The Time-varying Asymmetric Barrier Lyapunov Function (TABLF) is embedded into the controllers for handling the time-varying asymmetric slip ratio constraint problems. Two adaptive nonlinear control methods (TABLF1 and TABLF2) based on TABLF are proposed not only to track the optimal slip ratio but also to guarantee no violation on the slip ratio constraints. Simulation results show that the proposed controllers can guarantee no violation on slip ratio constraints and avoid self-locking. In the meantime, TABLF1 controller can achieve a faster convergence rate, shorter stopping time, and shorter distance, compared to TABLF2 controller with the same control parameters.

1. Introduction

An Antilock Braking System (ABS) is one of the main vehicle active safety devices and it has a function to avoid vehicle wheels self-locking, to shorten braking distance, to ensure the lateral stability according to the regulated wheel slip ratio. The basic objective of ABS is to regulate wheel slip at its optimum value while maximizing longitudinal tire-runway friction to generate large lateral force. Many ABS control algorithms were developed in the past.

Traditional ABS control algorithms are based on wheel acceleration. One example of such algorithms is logic threshold method [1], in which slip ratio and acceleration are the first and second control thresholds, respectively. However, this method heavily depends on various parameters that need to be determined by experience or experiment. As a result, it is difficult to evaluate the stability of the system.

In recent years ABS based on the slip ratio control algorithm has much attention because of its better control performance. The main objective of the slip control is to regulate wheel slip at its optimum value for ensuring that the vehicle braking system has a maximum tire-road friction. Many theoretical studies have been conducted on slip ratio control algorithms, including combined control [2, 3], adaptive control [4, 5], nonlinear control [6], extremum seeking control [7, 8], sliding-mode control methods [9–12], fuzzy/neural network controls [13, 14], feedback control [15], and reinforcement Q-learning [16, 17]. Although these control algorithms have improved the response time and received the better slip ratio tracking performance, there are some limitations in these algorithms. The fuzzy control algorithm relies heavily on the staffs' experience. Therefore, it is hard to determine and debug the relevant parameters. As to the sliding-mode control algorithm, the existence of chatter problems restricts its application. The neural network control algorithm and reinforcement Q-learning algorithm are burdened with high data rate and complex arithmetic.

All the above control algorithms are mainly focused on how to track the optimum slip ratio with a good dynamic performance without considering how to fundamentally avoid slip rate working in unstable areas. However, in practice, the optimal slip rate varies with the change of pavement, especially on abrupt or uneven pavement. When the slip rate changes instantaneously, the existing control algorithm cannot guarantee that ABS works absolutely in the stable region, which will result in vehicle sideslip or tail flick.

Therefore, the ideal ABS system requires avoiding working in unstable areas fundamentally. In fact, there are healthy region, light slip region, and deep slip region according to the relationship between the slip ratio and the combination coefficient in braking operating region [18]. When a slip ratio controller works in the deep slip region, the ABS system is unable to obtain the maximum tire-road friction and the system would be self-locking in worst cases. Since road adhesion force depends on the normal force between the tire and the road surface, the normal force on the wheel is directly affected by the road roughness, thus influencing the braking performance of ABS on an uneven road. In this special case, the optimal slip ratio constraint boundaries will change with the variation of road. In other words, the optimal slip ratio constraint boundaries are time-varying. Therefore, it is important to address a constrained control algorithm of time-varying slip ratio for ensuring that the system output does not violate the time-varying constraints and that the vehicle works in a stable region.

Constrained control algorithms have been investigated, including a governor method [19, 20] and a model predictive controller [21, 22]. Different from these methods, Barrier Lyapunov Function (BLF) will become infinity when the variable approaches the constrained boundary. In view of this characteristic, BLF has been widely applied to state constraint and output constraint problems [23–26] in the area of general control theory and has achieved good tracking performance without violation on constraints. In recent years, constrained control algorithms based on BLF have been studied extensively [27–32]. In [31], an adaptive fuzzy NN control algorithm has been proposed for an uncertain constrained robot with unknown dynamics and constraints. Control design with output constraint and control design with all state constraints were proposed for constrained robots. A tan-type BLF had been employed to handle the effect of constraint. The uncertain dynamics of robots had been approximated online by using the learning capability from the fuzzy NN structure. In [32], a cooperative control method has been investigated for a nonuniform gantry crane system with constrained tension. A novel integral-Barrier Lyapunov Function was proposed to keep the tension values remaining in the constrained space. The system parameter uncertainties have been handled by two adaption laws. However, the time-varying constraint bounds are not considered in [31, 32]. In [33, 34], the constraint control methods based on BLF are adopted to avoid the slip rate working in the unstable region in aircraft landing system. But, because the working condition of the aircraft landing system is relatively single, neither the time-varying slip rate constraint control nor the uncertainty caused by modeling errors and external disturbances are considered in these two papers. However, the working condition of vehicle is more complex than that of aircraft, especially on abrupt or uneven pavement.

Motivated by above literatures, two adaptive time-varying constraint control methods based on Time-varying Asymmetric Barrier Lyapunov Function (TABLF) are proposed to solve the optimum slip ratio tracking problem. The main contributions of this paper include the following:

(1) We concern with a constraint control problem with time-varying asymmetric slip ratio constraints in an ABS, which fundamentally avoids the ABS working in the unstable region and ensures the stability and safety in the braking process.

(2) TABLF is introduced into the design process of the constrained controller to realize time-varying slip rate constrained control, and the system uncertainties are considered to improve system robustness of the algorithm.

(3) Simulations demonstrate the effectiveness of our TABLF control algorithm over the Quadratic Lyapunov Function (QLF) control algorithm.

The rest of this paper is organized as follows. In Section 2, the vehicle dynamic mode and an antilock system are described and discussed. Sections 3 and 4 introduce Barrier Lyapunov Function and the design of the adaptive time-varying asymmetric wheel slip constrained controllers. The wheel slip constrained controllers are evaluated through the simulations in Section 5, followed by some concluding remarks in Section 6.

2. System Dynamics

2.1. A Quarter Car Model. To simplify the system model, this paper neglects the secondary factors and makes some assumptions as follows:

(1) The tires are rigid.

(2) The system ignores the influence of the lateral wind.

A quarter car model [35] that holds the necessary characteristics of the whole vehicle was selected in this paper. The free body diagram of the quarter car model is shown in Figure 1. The force balance equation [35] in the longitudinal direction is

$$m\dot{v} = -\mu(\lambda) mg - c_v v^2 \tag{1}$$

$$J\dot{\omega} = r\mu(\lambda) mg - rf_\omega - T_b \tag{2}$$

where $m = 1/4$ vehicle mass, v = linear velocity of vehicle, $\mu(\lambda)$ = coefficient of friction between road and tyre which is nonlinear function of slip ratio and road dynamics, c_v = aerodynamics drag coefficient, J = the moment of inertia of the wheel, ω = the angular velocity of the wheel, r = the radius of the wheel, f_ω = viscous wheel friction force ($f_\omega = c\omega$, where c is coefficient of viscous friction), T_b = the braking torque acting on the wheel, and λ = wheel slip ratio that is ratio of difference of wheel and vehicle velocity to maximum velocity among the two velocities.

In the ABS controller design, due to the existence of the plant uncertainties and measured noise, the stability of the closed-loop control system is affected. Thus, to assess the robustness of the controller, we consider the plant uncertainties and unmodeled dynamics. Equations (1) and (2) can be rewritten as

$$m\dot{v} = -\mu(\lambda) mg - c_v v^2 + \Delta_1(t) \tag{3}$$

$$J\dot{\omega} = r\mu(\lambda) mg - rf_\omega - T_b + \Delta_2(t) \tag{4}$$

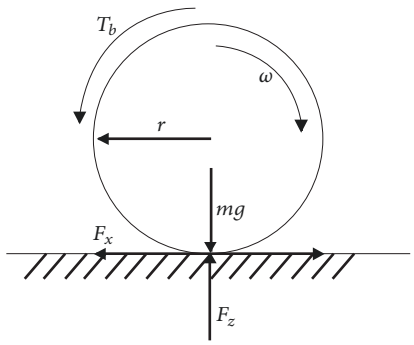

Figure 1: Free body diagram of the quarter car model.

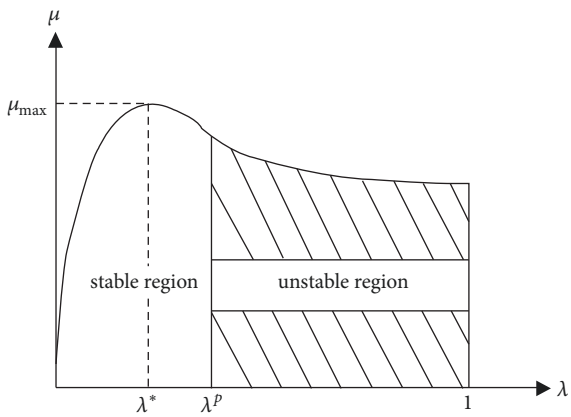

Figure 2: The relationship between friction coefficient and wheel slip.

where $\Delta_1(t)$ and $\Delta_1(t)$ include the uncertainty parameter deviation, external disturbance, and uncertain model error influencing on the stability of the system.

The wheel slip λ is defined as

$$\lambda = \frac{v - \omega r}{v} \times 100\% \tag{5}$$

Differentiating (5), we can obtain

$$\dot{\lambda} = \frac{(1-\lambda)\dot{v} - r\dot{\omega}}{v} \tag{6}$$

Substituting (3) and (4) into (6), we have

$$\begin{aligned}\dot{\lambda} = -\frac{1}{v}\Bigg(&\frac{r^2\mu(\lambda)mg}{J} - \frac{r^2 f_\omega}{J} + (1-\lambda)\mu(\lambda)g \\ &+ (1-\lambda)\frac{cv^2}{m}\Bigg) + \frac{T_b r}{vJ} + \frac{(1-\lambda)\Delta_1(t)}{mv} - \frac{r\Delta_2(t)}{vJ}\end{aligned} \tag{7}$$

2.2. Burckhardt's Tire Model and Problem Definition. There is a high nonlinear relationship between slip ratio λ and road adhesion coefficient $\mu(\lambda)$, which depends not only on the tire model but also on the road conditions. In this paper, the tire friction model introduced by Burckhardt [36] has been used to simulate an antilock brake system.

$$\mu(\lambda) = c_1\left(1 - e^{-c_2\lambda}\right) - c_3\lambda \tag{8}$$

$$\begin{aligned}\lambda_k &= \frac{1}{c_2}\log\frac{c_1c_2}{c_3} \\ \mu(\lambda_k) &= c_1 - \frac{c_3}{c_2}\left(1 - \log\frac{c_1c_2}{c_3}\right)\end{aligned} \tag{9}$$

where c_1 is the maximum value of the friction curve, c_2 is the shape of the friction curve, c_3 is the difference between the maximum value and the value at $\lambda = 1$ of the friction curve. λ_k is the maximum slip ratio, $\mu(\lambda_k)$ is the maximum adhesion coefficient. Different values of these parameters may denote different ground-contact friction conditions. Table 1 shows the parameters of the friction model for different runway surfaces.

Table 1: Friction model parameters.

Surface conditions	c_1	c_2	c_3
Dry asphalt	1.2801	23.9900	0.5200
Wet asphalt	0.8570	33.800	0.3470
Dry concrete	1.1973	25.168	0.5373
Snow	0.1946	94.1290	0.0646
Ice	0.0500	306.3900	0.0010

Figure 2 shows the relationship between friction coefficient and wheel slip.

The entire wheel slip range is divided into two regions according to the road surface adhesion coefficient curve: the stable region and the unstable region [37]. If the wheel slip is located in the unstable region due to the brake torque, which is bigger than the ground brake torque, then the wheel speed decreases, the slip ratio increases, and the ground brake force decreases continuously, until the vehicle wheel was locked. Consequently, the purpose of the proposed control scheme based on TABLF is to constrain wheel slip ratio in the stable region throughout the vehicle braking process.

Defining state variable $x = \lambda$, input variable $u = T_b$, and output variable y, the Antilock Braking System of vehicles can be rewritten as

$$\begin{aligned}\dot{x} &= f(x) + g(x)u + d(t) \\ y &= x\end{aligned} \tag{10}$$

where $f(x) = -(1/v)(r^2\mu(x)mg/J - r^2 f_w/J + (1-x)\mu(x)g + (1-x)(cv^2/m))$, $g(x) = r/vJ$, $d(t) = (1-\lambda)\Delta_1(t)/mv - r\Delta_2(t)/vJ$, and $|d(t)|$ is upper bound, but the bound is unknown.

The control objective for a nonlinear dynamic system is to determine an output feedback control system such that the output y can track a desired trajectory $y_d(t)$ while ensuring that all the closed-loop signals are bounded and that the output constraints are not violated. Furthermore, the constraint controller based on BLF is designed to suppress the total disturbances in slip dynamics to improve the ABS system robustness.

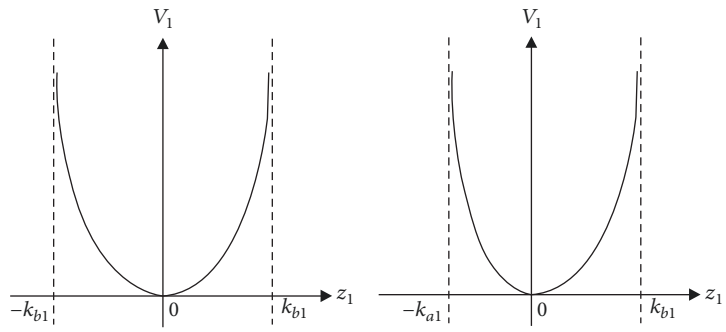

Figure 3: Symmetric (left) and an Asymmetric (right) Barrier Lyapunov Function.

3. Barrier Lyapunov Function Preliminaries

For establishing constraint satisfaction and performance bounds, the following definitions, assumptions, and Lemma 4 (see [23]) are necessary.

Definition 1 (see [24]). A Barrier Lyapunov Function is a scalar function $V(x)$, defined with respect to the system $\dot{x} = f(x,t)$ on an open region D containing the origin, that is continuous, positive definite, has continuous first-order partial derivatives at every point of D, has the property $V(x) \longrightarrow \infty$ as x approaches the boundary of D, and satisfies $V(x) \leq b$, $\forall t \geq 0$, along the solution of $\dot{x} = f(x,t)$ for $x(0) \in D$ and some positive constant b.

A Barrier Lyapunov Function should be symmetric or asymmetric according to the boundary character, as shown in Figure 3.

Assumption 2 (see [26]). There exist constants $\underline{K}_{ci}$, $\overline{K}_{ci}$, $i = 0,1,2$, satisfying $\underline{k}_{c1}(t) \geq \underline{K}_{c0}$ and $\overline{k}_{c1}(t) \leq \overline{K}_{c0}$, and its time derivatives satisfy $|\underline{k}_{ci}^{(i)}| \geq \underline{K}_{ci}$, $|\overline{k}_{ci}^{(i)}| \leq \overline{K}_{ci}$, $i = 1,2, \forall t \geq 0$.

Assumption 3 (see [26]). There exist positive constants Y_1, Y_2 and functions $\underline{Y}_0(t)$, $\overline{Y}_0(t)$ satisfying $\underline{Y}_0(t) > \underline{k}_{c1}(t)$, $\overline{Y}_0(t) < \overline{k}_{c1}(t)$, such that the desired trajectory $y_d(t)$ and its time derivatives satisfy $\underline{Y}_0(t) \leq y_d(t) \leq \overline{Y}_0(t)$ and $|\dot{y}_d(t)| \leq Y_1$, $|\ddot{y}_d(t)| \leq Y_2$, $\forall t \geq 0$, implying that they are continuous and available in a compact set $\Omega_{yd} := \{[y_d, \dot{y}_d, \ddot{y}_d]^T : y_d^2 + \dot{y}_d^2 + \ddot{y}_d^2 \leq \delta_{yd}\} \subset \mathbb{R}^3$.

Lemma 4 (see [21]). *For any positive functions $k_{a1}(t)$, $k_{b1}(t)$, let $\mathbf{S_1} = \{S_1 \in \mathbb{R} \mid -k_{a1}(t) < S_1 < k_{b1}(t)\} \subset \mathbb{R}$, and $N := \mathbb{R}^l \times \mathbf{S_1} \subset \mathbb{R}^{l+1}$ be open sets. Consider the system*

$$\dot{\eta} = h(t,\eta) \tag{11}$$

where $\eta := [\omega \ S_1]^T \in N$ and $h := \mathbb{R}_+ \times N \longrightarrow \mathbb{R}^{l+1}$ is piecewise continuous with respect to t and locally Lipschitz with respect to η, uniformly with respect to t, on $\mathbb{R}_+ \times N$. Suppose that there exist functions $U : \mathbb{R}^l \longrightarrow \mathbb{R}_+$ and $V_1 : \mathbf{S_1} \longrightarrow \mathbb{R}_+$ continuously differentiable and positive definite in their respective domains, such that

$$\begin{gathered} V_1(z) \longrightarrow \infty \quad \text{as } z \longrightarrow -k_{a1}(t) \text{ or } z \longrightarrow k_{b1}(t) \\ \gamma_1(\|\omega\|) \leq \mathrm{U}(\omega) \leq \gamma_2(\|\omega\|) \end{gathered} \tag{12}$$

where γ_1 and γ_2 are class K_∞ functions. Let $V(\eta) := V_1(S_1) + U(\omega)$ and $S_1(0) \in \mathbf{S_1}$. If the inequality holds

$$\dot{V} = \frac{\partial V}{\partial \eta} h \leq -cV + \nu \tag{13}$$

in the set $\eta \in N$ and c, ν are positive constants, then $S_1(t)$ remains in the open set $\mathbf{S_1}$, $\forall t \in [0,\infty]$.

4. Controller Design

In this section, slip ratio constraints are directly integrated into the controller design process to guarantee the constraints are not violated. We employ the Time-varying Asymmetric Barrier Lyapunov Function to design the controller.

Define the tracking error as

$$S(t) = y - y_d(t) \tag{14}$$

Define the time-varying output constraints $k_a(t)$, $k_b(t)$ as

$$\begin{aligned} k_a(t) &= y_d(t) - \underline{k}_c(t) \\ k_b(t) &= \overline{k}_c(t) - y_d(t) \end{aligned} \tag{15}$$

where $\underline{k}_c(t)$ is the time-varying lower bound of slip rate constraint, $\overline{k}_c(t)$ is the time-varying upper bound of slip rate constraint.

4.1. Time-Varying Constraint Backstepping Controller 1. We choose the Time-varying Asymmetric Barrier Lyapunov Function as

$$\begin{aligned} V = {} & \frac{1}{2}(1 - q(S)) \log \frac{k_a^2(t)}{k_a^2(t) - S_1(t)^2} \\ & + \frac{1}{2} q(S) \log \frac{k_b^2(t)}{k_b^2(t) - S_1(t)^2} + \frac{1}{2\gamma} \tilde{k}_2^2 \end{aligned} \tag{16}$$

where

$$q(S) = \begin{cases} 1, & 0 < S(t) < k_b(t) \\ 0, & -k_a(t) < S(t) \le 0 \end{cases} \tag{17}$$

$k_a(t)$ and $k_b(t)$ are the time-varying constraints on S_1, which can be set independently according to the upper and lower bounds of the desired trajectory $y_d(t)$, $\tilde{k}_2 = k_2 - \hat{k}_2$, $\hat{k}_2$ is the estimate of uncertainty upper bound k_2 and $k_2 \ge |d(t)|$, and γ is a positive constant.

Let $\mathbf{S} := \{S \in \mathbb{R} : -k_a(t) < S < k_b(t)\} \in \mathbb{R}$. By Assumptions 2 and 3, there exist positive constants $\underline{k}_b$, $\overline{k}_b$, $\underline{k}_a$, $\overline{k}_a$ such that

$$\begin{aligned} &\underline{k}_a < k_a(t) < \overline{k}_a, \\ &\underline{k}_b < k_a(t) < \overline{k}_b, \\ &\qquad \forall t \ge 0. \end{aligned} \tag{18}$$

Note. (1) It is clear that for any $S(t) \in (-k_a(t), k_b(t))$, $V(S(t)) \ge 0$ and only if $S(t) = 0$ we have $V(S(t)) = 0$. It implies that $V(S(t))$ is positive definite, because $\dot{V}(S(t))$ is continuous within each of the two intervals $S(t) \in (-k_a(t), 0)$ and $S(t) \in (0, k_b(t))$, respectively. Meanwhile, we have $\lim_{S\longrightarrow 0^+}(dV/dS) = \lim_{S\longrightarrow 0^-}(dV/dS) = 0$. It implies that $V(S(t))$ is continuously differentiable. Thus, V is a valid Lyapunov function candidate.

(2) When $k_a(t)$ and $k_b(t)$ are constants, the output constraints should be extended to be static constraints. When $k_a(t) = k_b(t)$, the time-varying asymmetric barrier function can be extended to time-varying symmetric barrier function, so the time-varying asymmetric barrier function affords greater flexibility on initial output conditions.

Differentiating (16), we can obtain

$$\begin{aligned} \dot{V} = {} & (1-q)\frac{S(t)\left(\dot{S}(t) - \left(\dot{k}_a(t)/k_a(t)\right)S(t)\right)}{k_a(t)^2 - S(t)^2} \\ & + q\frac{S(t)\left(\dot{S}(t) - \left(\dot{k}_b(t)/k_b(t)\right)S(t)\right)}{k_b(t)^2 - S(t)^2} + \frac{1}{\gamma}\tilde{k}_2\dot{\tilde{k}}_2 \end{aligned} \tag{19}$$

From (17), we have $q = 0$ and $1 - q = 1$ when $-k_a(t) < S(t) \le 0$. Equation (19) can be rewritten as

$$\dot{V} = S(t)\frac{1-q}{k_a^2(t) - S(t)^2}\left(\dot{S}(t) - \frac{\dot{k}_a(t)}{k_a(t)}S(t)\right) + \frac{1}{\gamma}\tilde{k}_2\dot{\tilde{k}}_2 \tag{20}$$

From (17), we have $q = 1$ and $1 - q = 0$ when $0 < S(t) < k_b(t)$. Rewriting (19) yields

$$\dot{V} = S(t)\frac{q}{k_b^2(t) - S(t)^2}\left(\dot{S}(t) - \frac{\dot{k}_b(t)}{k_b(t)}S(t)\right) + \frac{1}{\gamma}\tilde{k}_2\dot{\tilde{k}}_2 \tag{21}$$

According to (20) and (21), we have

$$\begin{aligned} \dot{V} = {} & S(t)\left(\frac{1-q}{k_a^2(t) - S(t)^2} + \frac{q}{k_b^2(t) - S(t)^2}\right)\left(\dot{S}(t)\right. \\ & \left. - (1-q)\frac{\dot{k}_a(t)}{k_a(t)}S(t) - q\frac{\dot{k}_b(t)}{k_b(t)}S(t)\right) + \frac{1}{\gamma}\tilde{k}_2\dot{\tilde{k}}_2 \\ = {} & S(t)\left(\frac{1-q}{k_a^2(t) - S(t)^2} + \frac{q}{k_b^2(t) - S(t)^2}\right)\left(f(x)\right. \\ & + g(x)u - \dot{y}_d + d(t) - (1-q)\frac{\dot{k}_a(t)}{k_a(t)}S(t) \\ & \left. - q\frac{\dot{k}_b(t)}{k_b(t)}S(t)\right) + \frac{1}{\gamma}\tilde{k}_2\dot{\tilde{k}}_2 \end{aligned} \tag{22}$$

Set $\theta = (1-q)/(k_a^2(t) - S(t)^2) + q/(k_b^2(t) - S(t)^2)$ and we have $\theta > 0$.

The adaptive controller is designed as

$$\begin{aligned} u = {} & \frac{1}{g(x)}\left\{-f(x) + \dot{y}_d(t) - \left[k_1 + \overline{k}_1(t)\right]S(t)\right. \\ & \left. - \hat{k}_2 \operatorname{sign}(S(t))\right\} \end{aligned} \tag{23}$$

where k_1 is a positive constants; the time-varying gain $\overline{k}_1(t)$ is given by

$$\overline{k}_1(t) = \sqrt{(1-q)\left(\frac{\dot{k}_a(t)}{k_a(t)}\right)^2 + q\left(\frac{\dot{k}_b(t)}{k_b(t)}\right)^2 + \beta} \tag{24}$$

where $\beta \ge 0$.

The adaptive law is designed as follows:

$$\dot{\hat{k}}_2 = \gamma\theta|S(t)| \tag{25}$$

Remark 5. Let $\overline{K}_1(t) = \overline{k}_1(t) + (1-q)(\dot{k}_a(t)/k_a(t)) + q(\dot{k}_b(t)/k_b(t))$. β can guarantee $\overline{K}_1(t) \ge 0$ when $\dot{k}_a(t)$ and $\dot{k}_b(t)$ are both zero.

Setting $\overline{K}_1(t) = \overline{k}_1(t) + (1-q)(\dot{k}_a(t)/k_a(t)) + q(\dot{k}_b(t)/k_b(t))$ and substituting (23), (24), and (25) into (22), we can obtain

$$\begin{aligned} \dot{V} = {} & S(t)\theta\left\{-\left[k_1 + \overline{k}_1(t) + (1-q)\frac{\dot{k}_a(t)}{k_a(t)} + q\frac{\dot{k}_b(t)}{k_b(t)}\right]\right. \\ & \left. \cdot S(t) + d(t) - \hat{k}_2 \operatorname{sign}(S(t))\right\} + \frac{1}{\gamma}\tilde{k}_2\dot{\tilde{k}}_2 = S(t) \\ & \cdot \theta\left[-\left(k_1 + \overline{K}_1(t)\right)S(t) + d(t) - \hat{k}_2 \operatorname{sign}(S(t))\right. \\ & \left. + \tilde{k}_2 \operatorname{sign}(S(t))\right] + \frac{1}{\gamma}\tilde{k}_2\dot{\tilde{k}}_2 = -\theta\left(k_1 + \overline{K}(t)\right)S(t)^2 \\ & - \theta\left(k_2|S(t)| - S(t)d(t)\right) + \theta\tilde{k}_2|S(t)| + \frac{1}{\gamma}\tilde{k}_2\dot{\tilde{k}}_2 \\ & \le -\theta\left(k_1 + \overline{K}(t)\right)S(t)^2 - \theta\left(k_2|S(t)| - |S(t)|\right. \\ & \left. \cdot |d(t)|\right) + \tilde{k}_2\left(\theta|S(t)| + \frac{1}{\gamma}\dot{\tilde{k}}_2\right) \le -\theta\left(k_1 + \overline{K}(t)\right) \\ & \cdot S(t)^2 \end{aligned} \tag{26}$$

According to (26), $\dot{V}$ is negative definite when the control law is (23), and the Time-varying Asymmetric Barrier Lyapunov Function is (16). The system is asymptotically stable based on Barbalat's lemma [21]. $S(t)$ is guaranteed to converge to zero asymptotically.

4.2. Time-Varying Constraint Backstepping Controller 2. In Section 4.1, we have the following results:

$$\begin{aligned}\dot{V} = S(t)\theta\Big(& f(x) + g(x)u - \dot{y}_d + d(t) \\ & - (1-q)\frac{\dot{k}_a(t)}{k_a(t)}S(t) - q\frac{\dot{k}_b(t)}{k_b(t)}S(t)\Big) + \frac{1}{\gamma}\tilde{k}_2\dot{\tilde{k}}_2\end{aligned} \tag{27}$$

The adaptive controller is designed as

$$\begin{aligned}u = \frac{1}{g(x)}\Big\{& -f(x) + \dot{y}_d(t) \\ & - k_1\left[(1-q)\left(k_a^2(t) - S(t)^2\right) + q\left(k_b^2(t) - S(t)^2\right)\right] \\ & \cdot S(t) + \overline{k}_1(t)S(t) - \widehat{k}_2 \operatorname{sign}(S(t))\Big\}\end{aligned} \tag{28}$$

where k_1 is a positive constants; the time-varying gain $\overline{k}_1(t)$ is given by

$$\overline{k}_1(t) = (1-q)\frac{\dot{k}_a(t)}{k_a(t)} + q\frac{\dot{k}_b(t)}{k_b(t)} \tag{29}$$

The adaptive law is designed as follows:

$$\dot{\widehat{k}}_2 = \gamma\theta|S(t)| \tag{30}$$

Substituting (28), (29), and (30) into (27), we can obtain

$$\begin{aligned}\dot{V} = S(t)\theta\Big[& -k_1\left[(1-q)\left(k_a^2(t) - S(t)^2\right)\right. \\ & \left. + q\left(k_b^2(t) - S(t)^2\right)\right]S(t) + \overline{k}_1(t)S(t) - (1-q) \\ & \cdot \frac{\dot{k}_a(t)}{k_a(t)}S(t) - q\frac{\dot{k}_b(t)}{k_b(t)}S(t) + d(t) - \widehat{k}_2 \operatorname{sign}(S(t))\Big] \\ & + \frac{1}{\gamma}\tilde{k}_2\dot{\tilde{k}}_2 = -k_1S(t)^2 + S(t)\theta\left[d(t) - k_2 \operatorname{sign}(S(t))\right. \\ & \left. + \tilde{k}_2 \operatorname{sign}(S(t))\right] + \frac{1}{\gamma}\tilde{k}_2\dot{\tilde{k}}_2 = -k_1S(t)^2 \\ & - \theta\left[k_2|S(t)| - S(t)d(t)\right] + \theta\tilde{k}_2|S(t)| + \frac{1}{\gamma}\tilde{k}_2\dot{\tilde{k}}_2 \\ & \le -k_1S(t)^2 - \theta\left[k_2|S(t)| - |S(t)||d(t)|\right] \\ & + \tilde{k}_2\left[\theta|S(t)| + \frac{1}{\gamma}\dot{\tilde{k}}_2\right] \le -k_1S(t)^2\end{aligned} \tag{31}$$

Remark 6. From (17), we have $q = 0$ and $1 - q = 1$ when $-k_a(t) < S(t) \le 0$. We have

$$\begin{aligned}& S(t)\theta\left\{-k_1\left[(1-q)\left(k_a^2(t) - S(t)^2\right)S(t)\right.\right. \\ & \left.\left. + kq\left(k_b^2(t) - S(t)^2\right)\right]S(t)\right\} = S(t) \\ & \cdot \frac{1-q}{k_a^2(t) - S(t)^2}\left[-k_1(1-q)\left(k_a^2(t) - S(t)^2\right)S(t)\right] \\ & = -k_1S(t)^2\end{aligned} \tag{32}$$

From (17), we have $q = 1$ and $1 - q = 0$ when $0 < S(t) < k_b(t)$. We have

$$\begin{aligned}& S(t)\theta\left\{-k_1\left[(1-q)\left(k_a^2(t) - S(t)^2\right)S(t)\right.\right. \\ & \left.\left. + kq\left(k_b^2(t) - S(t)^2\right)\right]S(t)\right\} = S(t) \\ & \cdot \frac{q}{k_b^2(t) - S(t)^2}\left[-k_1q\left(k_b^2(t) - S(t)^2\right)S(t)\right] \\ & = -k_1S(t)^2\end{aligned} \tag{33}$$

So we can have

$$\begin{aligned}& S(t)\theta\left\{-k_1\left[(1-q)\left(k_a^2(t) - S(t)^2\right)\right.\right. \\ & \left.\left. + q\left(k_b^2(t) - S(t)^2\right)\right]S(t)\right\} = -k_1S(t)^2\end{aligned} \tag{34}$$

According to (31), $\dot{V}$ is negative definite when the control law is (28), and the Time-varying Asymmetric Barrier Lyapunov Function is (16). The system is asymptotically stable based on Barbalat's lemma [21]. $S(t)$ is guaranteed to converge to zero asymptotically.

5. Simulation Analysis

In this section, we present the simulations study to illustrate the performance of the proposed controllers. To illustrate the effectiveness of our control algorithm, we compare it with the control algorithm based on QLF under the same parameter condition.

For system (10) and definition (14), consider the QLF candidates as follows:

$$V = \frac{1}{2}S(t)^2 + \frac{1}{2\gamma}\tilde{k}_2^2 \tag{35}$$

Differentiating (35), we can obtain

$$\begin{aligned}\dot{V} &= S(t)\dot{S}(t) + \frac{1}{\gamma}\tilde{k}_2\dot{\tilde{k}}_2 \\ &= S(t)\left[f(x) + g(x)u - \dot{y}_d(t) + d(t)\right] + \frac{1}{\gamma}\tilde{k}_2\dot{\tilde{k}}_2\end{aligned} \tag{36}$$

The adaptive QLF control law is designed as

$$u = \frac{1}{g(x)}\left[-f(x) + \dot{y}_d(t) - k_1S(t) - \widehat{k}_2 \operatorname{sign}(S(t))\right] \tag{37}$$

Table 2: Vehicle model parameters.

Description	Symbol	value
the moment of inertia of the wheel	J	$0.65\,kgm^2$
the radius of the wheel	r	$0.31\,m$
1/4 vehicle mass	m	$350\,kg$
gravitational constant	g	$9.8\,m/s^2$
aerodynamics drag coefficient	c_v	$0.595\,N/m^2/s^2$
coefficient of viscous friction	c	$2.1468 \times 10^{-6}\,Nms$

where k_1 is a positive constants and the adaptive control law is designed as follows:

$$\dot{\hat{k}}_2 = \gamma\,|S(t)| \tag{38}$$

Substituting (37) and (38) into (36), we have

$$\begin{aligned}\dot{V} &= S(t)\left[-k_1 S(t) + d(t) - \hat{k}_2 \operatorname{sign}(S(t))\right] + \frac{1}{\gamma}\tilde{k}_2\dot{\tilde{k}}_2 \\ &= -k_1 S(t)^2 \\ &\quad + S(t)\left[d(t) - k_2 \operatorname{sign}(S(t)) + \tilde{k}_2 \operatorname{sign}(S(t))\right] \\ &\quad + \frac{1}{\gamma}\tilde{k}_2\dot{\tilde{k}}_2 \\ &= -k_1 S(t)^2 - \left[k_2\,|S(t)| - S(t)\,d(t)\right] + \tilde{k}_2\,|S(t)| \\ &\quad + \frac{1}{\gamma}\tilde{k}_2\dot{\tilde{k}}_2 \\ &\le -k_1 S(t)^2 - \left[k_2\,|S(t)| - |S(t)|\,|d(t)|\right] \\ &\quad + \tilde{k}_2\left[|S(t)| + \frac{1}{\gamma}\dot{\tilde{k}}_2\right] \le -k_1 S(t)^2\end{aligned} \tag{39}$$

According to (39), $\dot{V}$ is negative definite when the control law is (37) and the Quadratic Lyapunov Function is (35). Thus, the system is stable.

To eliminate the chattering phenomenon, the saturation function (40) is used to replace the switching term sign($S(t)$ in the control law (23), (28), and (37).

$$sat\left(\frac{S(t)}{\varphi}\right) = \begin{cases} \operatorname{sign}\left(\dfrac{S(t)}{\varphi}\right), & |S(t)| > \varphi \\ \dfrac{S(t)}{\varphi}, & |S(t)| \le \varphi \end{cases} \tag{40}$$

where $\varphi = 0.2$.

The main parameters [35] of the vehicle model are showed in Table 2 for a controller simulation analysis.

Desired slip ratio for dry asphalt surface is $\lambda^* = 0.12$. From Table 1 we can have $c_1 = 1.2801$, $c_2 = 23.9900$, and $c_3 = 0.52$. In a way similar to [38], we use $0.02\sin(30t)$ as the influence of road roughness on slip rate. Thus, we have $\lambda(t)^* = 0.12 + 0.02\sin(30t)$. The uncertain parameters $\Delta_1(t) = 0.5 * \sin(t)$, $\Delta_2(t) = 0.5 * \sin(t)$.

The controller parameters are chosen as follows: $\overline{k}_c(t) = 0.144 + 0.024\sin(30t)$, $\underline{k}_c(t) = 0$. From formula (15), we can have $k_a(t) = 0.12 + 0.02\sin(30t)$, $k_b(t) = 0.024 + 0.004\sin(30t)$. The controller gain $k_1 = 190$, $\dot{\hat{k}}_2(0) = 0.8$, $\beta = 0.1$, $\gamma = 30$.

The initial conditions of the vehicle are $v(0) = 25.0015\,m/s$ and $w(0) = 80.65\,rad/s$, which implies $\lambda(0) = 0$. In order to avoid the singular value of slip rate at $v = 0$, we will stop simulation when $v = 0.1\,m/s$. The simulation results are shown in Figure 4.

The time-varying upper limit of the optimal slip rate is $\overline{k}_c(t) = 0.144 + 0.024\sin(30t)$ and the time-varying lower limit of the optimal slip rate is $\underline{k}_c(t) = 0$. The time-varying constrained range is represented by the yellow lines in Figure 4(a). The upper bound of tracking error constraint is $k_b(t) = 0.024 + 0.004\sin(30t)$ and the lower bound of tracking error constraint is $-k_a(t) = -(0.12 + 0.02\sin(30t))$. The time-varying tracking error constraint is represented by the yellow lines in Figure 4(b). From Figures 4(a) and 4(b), it can be seen that TABLF1 and TABLF2 controller can receive good tracking performance of slip ratio, the slip ratio stays strictly within the time-varying slip ratio constraint boundary $(\underline{k}_c(t), \overline{k}_t(t))$, and tracking error stays strictly within the error constraint boundary $(-k_a(t), k_b(t))$. This implies the ABS will provide the maximum braking force at its steady area. However, under the QLF controller, the slip ratio constraint boundary and error constraint boundary are violated when the ABS works at the high speed process, which means that the slip ratio is already in an unstable area and the heavy wheel skidding of vehicle occurs.

The reason for this phenomenon is that the Time-varying Asymmetric Barrier Lyapunov Function is adopted when we designed the controllers in this paper. Furthermore, the output variable is strictly within the bounds of constraints. Nevertheless, the output variable cannot be guaranteed within the bounds of constraints when the Quadratic Lyapunov Function is used.

Figures 4(c), 4(d), and 4(e) demonstrate the vehicle velocity and wheel velocity under different controllers. Compared with the QLF controller, the wheel speed of the TABLF has no oscillation. This can improve the vehicle ride comfort and stationarity. Figure 4(f) shows the stopping distance. From the stopping time and stopping distance, TABLF1 controller is superior to QLF controller, and QLF controller is superior to TABLF2 controller. But, by restricting the slip ratio, the slip ratio can be avoided in the unstable region and the stability of the vehicle braking system is improved in TABLF1 controller and TABLF2 controller. Figure 4(g) illustrates the braking torque. In contrast to the QLF controller, the braking torque of the TABLF1 controller and TABLF2 controller have no oscillation, which is helpful to prolong the lifespan of the actuator.

Table 3 shows the results of the TABLF1 controller, TABLF1 controller and QLF controller in the same parameters.

Table 4 shows the comparison results of the TABLF1 controller, TABLF1 controller and QLF controller in the same parameters.

Table 3: Results of three controllers.

	Convergence time	Stopping time	Stopping distance
QLF	0.3480s	2.1860s	27.13m
TABLF1	0.1200s	2.1720s	26.80m
TABLF2	0.4440s	2.2120s	27.50m

Table 4: Comparison results of three controllers.

	Violation constraint	Convergence rate	Stopping distance	Stopping time	Wheel speed oscillation
QLF	Y	faster	shorter	shorter	Y
TABLF1	N	fastest	shortest	shortest	N
TABLF2	N	slowest	longest	longest	N

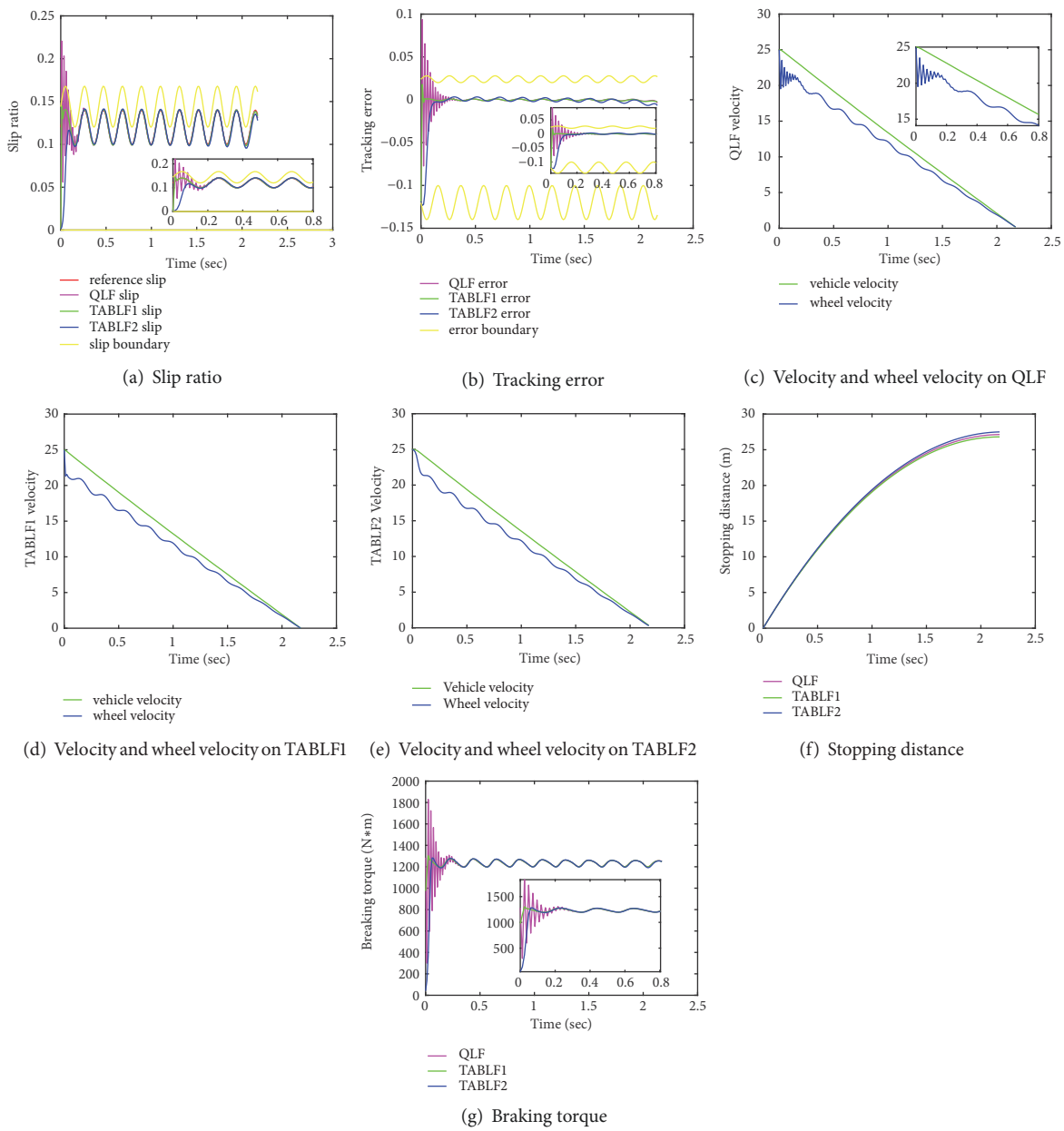

(a) Slip ratio (b) Tracking error (c) Velocity and wheel velocity on QLF

(d) Velocity and wheel velocity on TABLF1 (e) Velocity and wheel velocity on TABLF2 (f) Stopping distance

(g) Braking torque

Figure 4: Simulation results on time-varying constraint boundary.

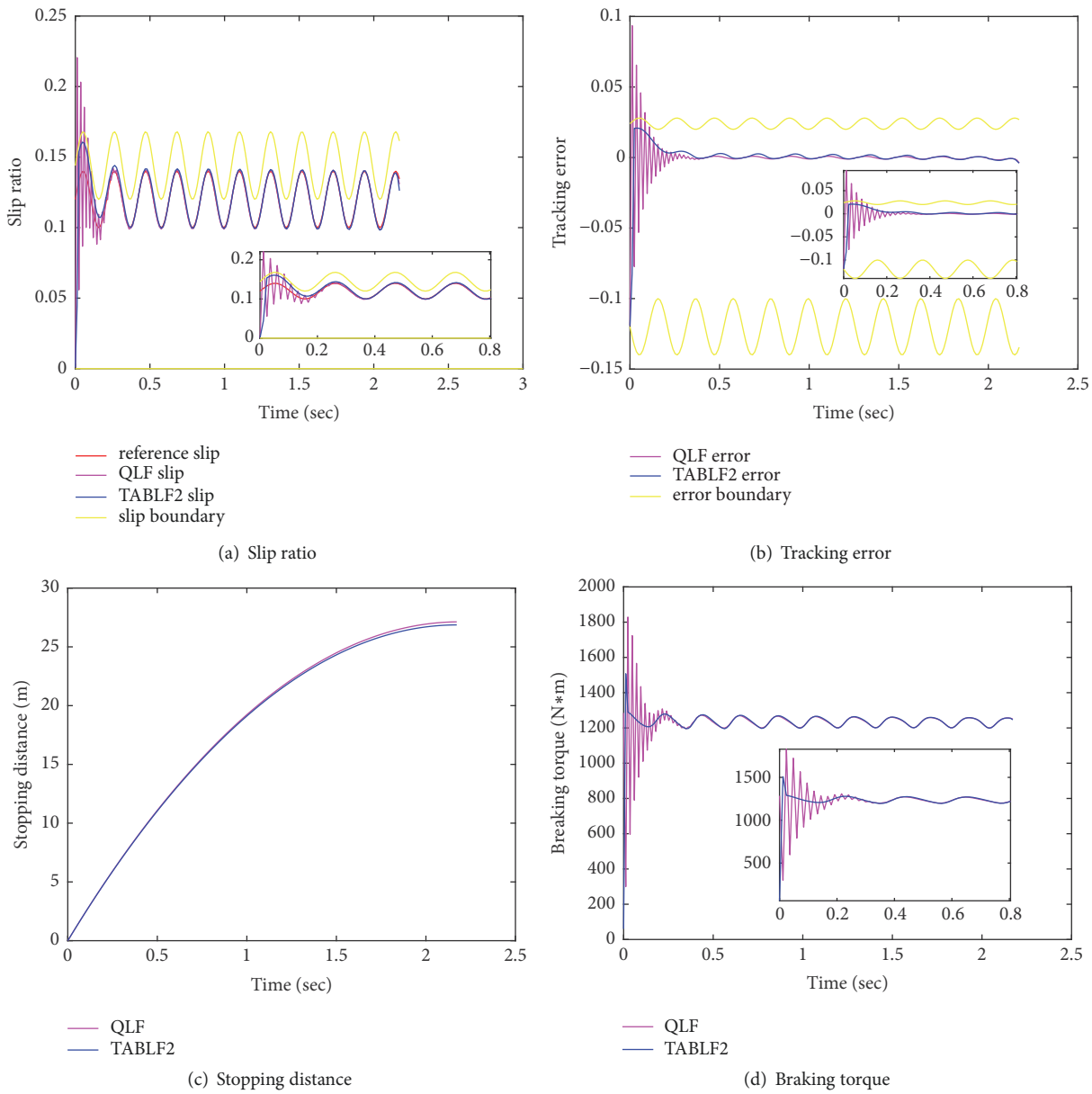

FIGURE 5: Simulation result of TABLF2 controller ($k_1 = 550$) and QLF controller ($k_1 = 190$) on time-varying constraint boundary.

In order to reduce the stopping time and stopping distance of the TABLF2 controller, we can increase the controller parameter k_1 to reduce the braking time without violating the constraint boundary. From formula (37), it can be seen that the overshoot of slip ratio of the QLF controller will be more serious with the increase of the parameter k_1. Therefore, we only contrasted TABLF2 controller whose parameter k_1 increased with the QLF controller whose parameter $k_1 = 190$. Figure 5 shows the comparison result of TABLF2 controller ($k_1 = 550$) and QLF controller ($k_1 = 190$) on time-varying constraint boundary.

From Figure 5, the TABLF2 controller receives the better tracking performance, the smoother braking torque, the shorter stopping time and stopping distance without violating the constraint boundary.

The stopping time is 2.1740s and stopping distance is 26.88m under the TABLF2 controller, while the stopping time is 2.1860s and stopping distance is 27.13m under the QLF controller.

6. Conclusions

In this paper, a quarter vehicle braking model with system uncertainties for ABS is proposed and two adaptive constraint controllers are designed based on TABLF to guarantee no violation on the slip ratio constraints such that the vehicle works in the stable region. The proposed controllers and the controller based on QLF are compared via simulations on the pavement of time-varying slip constraint boundaries. The

simulation results show that TABLF1 controller and TABLF2 controller can implement zero steady state error tracking of the wheel slip and can guarantee that the slip ratio constraint boundaries are not violated on different pavements. By contrast, the controller based on QLF causes the violation of the constraint boundary at high speeds. This means that the vehicle has worked in an unstable region. In the meantime, the proposed controllers can improve the vehicle ride comfort and stationarity and prolong the lifespan of the actuator because the wheel speed and the braking torque have no oscillation compared with the QLF controller. The simulation results also indicate that in the stopping time and stopping distance, TABLF1 controller is superior to QLF controller, and QLF controller is superior to TABLF2 controller with the same gain parameter. By increasing parameter k_1, the TABLF2 controller can have a shorter stopping time and stopping distance without violating the constraint boundary than the QLF controller.

Data Availability

The data contains some vehicle parameter data and control parameter data and some simulation graphics. The vehicle parameter data have been pointed out from the reference. The control parameter data are calculated based on control algorithm. All data included in this study are available upon request from corresponding author.

Conflicts of Interest

The authors declare that they have no conflicts of interest.

Acknowledgments

This work is supported by National Natural Science Fund of China (51775247), Jiangsu Province "Six Talent Peaks" Project (2015-XNYQC-004), Post Doctoral Fund in Jiangsu (1601031C), Jiangsu Province Road Transport Application Key Laboratory Fund (BM20082061506), and Research Start Fund of Jiangsu University (15JDG125).

References

[1] T. Zheng and F. Ma, "Automotive ABS control strategy based on logic threshold," *J. Traffic and Transportation Engineering*, vol. 10, pp. 69–74, 2010.

[2] W.-C. Lin, C.-L. Lin, P.-M. Hsu, and M.-T. Wu, "Realization of anti-lock braking strategy for electric scooters," *IEEE Transactions on Industrial Electronics*, vol. 61, no. 6, pp. 2826–2833, 2014.

[3] D. Capra, E. Galvagno, V. Ondrak, B. van Leeuwen, and A. Vigliani, "An ABS control logic based on wheel force measurement," *Vehicle System Dynamics*, vol. 50, no. 12, pp. 1779–1796, 2012.

[4] A. Badie Sharkawy, "Genetic fuzzy self-tuning PID controllers for antilock braking systems," *Engineering Applications of Artificial Intelligence*, vol. 23, no. 7, pp. 1041–1052, 2010.

[5] G. P. Incremona, E. Regolin, A. Mosca, and A. Ferrara, "Sliding mode control algorithms for wheel slip control of road vehicles," in *Proceedings of the 2017 American Control Conference, ACC 2017*, pp. 4297–4302, USA, May 2017.

[6] S. Mahanty and S. C. Subramanian, "A non-linear model-based slip controller for electropneumatic brakes in heavy commercial vehicles," *International Journal of Heavy Vehicle Systems*, vol. 20, no. 1, pp. 35–60, 2013.

[7] C. Zhang and R. Ordóñez, "Numerical optimization-based extremum seeking control with application to ABS design," *IEEE Transactions on Automatic Control*, vol. 52, no. 3, pp. 454–467, 2007.

[8] E. Dinçmen, B. A. Güvenç, and T. Acarman, "Extremum-seeking control of ABS braking in road vehicles with lateral force improvement," *IEEE Transactions on Control Systems Technology*, vol. 22, no. 1, pp. 230–237, 2014.

[9] E. Kayacan, Y. Oniz, and O. Kaynak, "A grey system modeling approach for sliding-mode control of antilock braking system," *IEEE Transactions on Industrial Electronics*, vol. 56, no. 8, pp. 3244–3252, 2009.

[10] B. Subudhi and S. S. Ge, "Sliding-mode-observer-based adapive slio ratio control for electric and hybird vehicles," *IEEE Transactions on Intelligent Transportation Systems*, vol. 13, no. 4, pp. 1617–1626, 2012.

[11] R. De Castro, R. E. Araujo, and D. Freitas, "Wheel slip control of EVs based on sliding mode technique with conditional integrators," *IEEE Transactions on Industrial Electronics*, vol. 60, no. 8, pp. 3256–3271, 2013.

[12] M. Alireza, H. Amir, and S. Masoudi, "Comparison of Adaptive Fuzzy Sliding-Mode Pulse Width Modulation Control With Common Model-Based Nonlinear Controllers for Slip Control in Antilock Braking," *Journal of Dynamic Systems Measurement and Control*, vol. 140, pp. 0110141–01101415, 2018.

[13] V. Ćirović and D. Aleksendrić, "Adaptive neuro-fuzzy wheel slip control," *Expert Systems with Applications*, vol. 40, no. 13, pp. 5197–5209, 2013.

[14] P. C. Zhang, H. W. He, H. Q. Guo, and J. K. Peng, "Multi-field modeling and simulation of ABS based on fuzzy control," *J. Beijing Institute of China*, vol. 23, pp. 66–71, 2014.

[15] H. Mirzaeinejad and M. Mirzaei, "A novel method for nonlinear control of wheel slip in anti-lock braking systems," *Control Engineering Practice*, vol. 18, no. 8, pp. 918–926, 2010.

[16] M. Radac, R. Precup, and R. Roman, "Anti-lock braking systems data-driven control using Q-learning," in *Proceedings of the 2017 IEEE 26th International Symposium on Industrial Electronics (ISIE)*, pp. 418–423, Edinburgh, United Kingdom, June 2017.

[17] M.-B. Radac and R.-E. Precup, "Data-driven model-free slip control of anti-lock braking systems using reinforcement Q-learning," *Neurocomputing*, vol. 275, pp. 317–329, 2018.

[18] P. E. Wellstead, "Analysis and redesign of an antilock brake system controller," *IEE Proceedings Control Theory and Applications*, vol. 144, no. 5, pp. 413–426, 1997.

[19] E. Gilbert and I. Kolmanovsky, "Nonlinear tracking control in the presence of state and control constraints: a generalized reference governor," *Automatica*, vol. 38, no. 12, pp. 2063–2073, 2002.

[20] K. Kogiso and K. Hirata, "Reference governor for constrained systems with time-varying references," *Robotics and Autonomous Systems*, vol. 57, no. 3, pp. 289–295, 2009.

[21] A. Bemporad, F. Borrelli, and M. Morari, "Model predictive control based on linear programming—the explicit solution," *IEEE Transactions on Automatic Control*, vol. 47, no. 12, pp. 1974–1985, 2002.

[22] C. Satzger, R. de Castro, and A. Knoblach, "Robust Linear Parameter Varying Model Predictive Control and its Application to Wheel Slip Control," *IFAC-PapersOnLine*, vol. 50, no. 1, pp. 1514–1520, 2017.

[23] B. Ren, S. S. Ge, K. P. Tee, and T. H. Lee, "Adaptive neural control for output feedback nonlinear systems using a barrier lyapunov function," *IEEE Transactions on Neural Networks and Learning Systems*, vol. 21, no. 8, pp. 1339–1345, 2010.

[24] K. P. Tee, S. S. Ge, and E. H. Tay, "Barrier Lyapunov functions for the control of output-constrained nonlinear systems," *Automatica*, vol. 45, no. 4, pp. 918–927, 2009.

[25] B. Niu and J. Zhao, "Barrier Lyapunov functions for the output tracking control of constrained nonlinear switched systems," *Systems & Control Letters*, vol. 62, no. 10, pp. 963–971, 2013.

[26] K. P. Tee, B. Ren, and S. S. Ge, "Control of nonlinear systems with time-varying output constraints," *Automatica*, vol. 47, no. 11, pp. 2511–2516, 2011.

[27] W. He, S. Zhang, and S. S. Ge, "Adaptive boundary control of a nonlinear flexible string system," *IEEE Transactions on Control Systems Technology*, vol. 22, no. 3, pp. 1088–1093, 2014.

[28] W. He, S. Zhang, and S. S. Ge, "Adaptive control of a flexible crane system with the boundary output constraint," *IEEE Transactions on Industrial Electronics*, vol. 61, no. 8, pp. 4126–4133, 2014.

[29] W. He and S. S. Ge, "Vibration control of a flexible beam with output constraint," *IEEE Transactions on Industrial Electronics*, vol. 62, no. 8, pp. 5023–5030, 2015.

[30] Y.-J. Liu and S. Tong, "Barrier Lyapunov functions for Nussbaum gain adaptive control of full state constrained nonlinear systems," *Automatica*, vol. 76, pp. 143–152, 2017.

[31] W. He and Y. Dong, "Adaptive fuzzy neural network control for a constrained robot using impedance learning," *IEEE Transactions on Neural Networks and Learning Systems*, vol. pp, no. 99, pp. 1–13, 2017.

[32] W. He and S. S. Ge, "Cooperative control of a nonuniform gantry crane with constrained tension," *Automatica*, vol. 66, pp. 146–154, 2016.

[33] Y. Qiu, X. Liang, and Z. Dai, "Backstepping dynamic surface control for an anti-skid braking system," *Control Engineering Practice*, vol. 42, pp. 140–152, 2015.

[34] X. Chen, Z. Dai, H. Lin, Y. Qiu, and X. Liang, "Asymmetric Barrier Lyapunov Function-Based Wheel Slip Control for Antilock Braking System," *International Journal of Aerospace Engineering*, vol. 2015, Article ID 917807, 10 pages, 2015.

[35] P. Chaudhari, V. Sharma, P. D. Shendge, and S. B. Phadke, "Disturbance observer based sliding mode control for anti-lock braking system," in *Proceedings of the 1st International Conference on Power Electronics, Intelligent Control and Energy Systems (ICPEICES)*, pp. 1–5, 2016.

[36] M. Burckhardt, *Fahrwerktechnik: Radschlupf-Regelsysteme*, vol. 16, Vogel-Verlag, Wurtzburg, Germany, 1993.

[37] D. Madau, F. Yuan, L. Davis, and L. Feldkamp, "Fuzzy logic anti-lock brake system for a limited range coefficient of friction surface," in *Proceedings of the [1993] Second IEEE International Conference on Fuzzy Systems*, pp. 883–888, San Francisco, CA, USA.

[38] M. Akbarzadeh-T, K. Emami, and N. Pariz, "Adaptive discrete-time fuzzy sliding mode control for anti-lock braking systems," in *Proceedings of the 2002 Annual Meeting of the North American Fuzzy Information Processing Society Proceedings*, pp. 554–559, New Orleans, LA, USA.

Advances in Operations Research
Advances in Decision Sciences
Journal of Applied Mathematics
The Scientific World Journal
Journal of Probability and Statistics
International Journal of Mathematics and Mathematical Sciences
Hindawi
Submit your manuscripts at
www.hindawi.com
Journal of Optimization
International Journal of Engineering Mathematics
International Journal of Analysis
Journal of Complex Analysis
Advances in Numerical Analysis
Mathematical Problems in Engineering
International Journal of Differential Equations
Discrete Dynamics in Nature and Society
International Journal of Stochastic Analysis
Journal of Mathematics
Journal of Function Spaces
Abstract and Applied Analysis
Advances in Mathematical Physics